Theoretical Study on Electronic and Solvent Reorganization Associated with a Charging Process of Organic Compounds. 2. A New Decomposition Procedure into Electrostatic and Nonelectrostatic Responses

Hirofumi Sato,[†] Yasuhiro Kobori,[‡] Shozo Tero-Kubota,[‡] and Fumio Hirata*[,§]

Department of Molecular Engineering, Kyoto University, Yoshida, Kyoto, 606-8501, Japan, Institute of Multidisciplinary Research for Advanced Materials, Tohoku University, Katahira 2-1-1, Aobaku, Sendai, 980-8577, Japan, and Department of Theoretical Studies, Institute for Molecular Science and School of Mathematical and Physical Science, The Graduate University for Advanced Studies, Okazaki 444-8585, Japan

Received: October 17, 2003; In Final Form: May 14, 2004

A new procedure, which enables us to decompose the solvent reorganization energy into electrostatic and nonelectrostatic contributions, is proposed. By using the procedure proposed by us very recently (*J. Phys. Chem. A* **2002**, *106*, 2300−2304), the solvent reorganization process and electronic structures of *N*,*N*-dimethylaniline (DMA) and 1,4-dimethoxybenzene (DMB) associated with a charging process in acetonitrile solution are studied at the molecular level on the basis of the ab initio reference interaction site model−self-consistent field (RISM−SCF) method. Differences as well as similarities between the solvation processes of the two molecules are discussed on the basis of the newly proposed method.

1. Introduction

Numerous studies have been done in charge transfer (CT) reactions due to their essential roles played in a variety of chemical, physical, and biological processes.[1] It is the solvent reorganization energy λ_s that characterizes the CT process in solution, because it is concerned with the rate constant according to the Marcus theory. In the theory, λ_s can be evaluated from three parameters; dielectric constant of solvent, the "radius" of donor and acceptor, and the separation between the redox pair. Given the parameters adequately adjusted, the theory, indeed, is valid for extensive solute−solvent systems. Accurate measurements of λ_s were carried out very recently by Kobori et al.[2] with a new technique based on the time-resolved electron paramagnetic resonance (TR-EPR). Their report shows that the Marcus theory provides a good description for the process in a variety of solute−solvent systems, if "radii" of the redox pair are properly adjusted.

The "radius" is a single parameter that embodies molecular nature in the Marcus theory. However, the description in terms of "radius" is too poor to characterize intriguing chemistry of the solvent reorganization associated with the CT process. For example, molecular detail of solvent reorganization and the electronic-structure change in solute do not appear in the theory. More importantly, the Marcus theory relies basically on an approximation in which only the electrostatic interaction between solute and solvent governs solvent fluctuation. It has been established that the solvent structure is generally determined by two types of interactions, the electrostatic and nonelectrostatic ones. Although these two interactions give good account of the solvation characteristics, it is not trivial to evaluate the contributions, especially for a realistic molecular system. Theoretical calculations of solvent reorganization energy λ_s for a polyatomic molecule are also very limited compared to simple atomic (spherical) systems.[3−7] A treatment beyond the Marcus theory based on the statistical mechanics for a polyatomic system is highly desired to study the physics and the molecular origin of λ_s.

The respective contribution from the donor or acceptor to the λ_s is in the same situation. This is because solvent reorganization energy is essentially a thermodynamic quantity, and an accurate estimation of free energy difference is required between the two states with different charge distributions. Characterization of the charge distribution of a solute is trivial for a simple atomic ion, but it is not the case for a polyatomic molecule. The charge distribution is determined essentially by the electronic structure that should be calculated by means of quantum chemistry. The calculation is by no means trivial, because the solute is subjected to the strong field from the solvent. A problem is then how to generate an appropriate ensemble of solvent configurations with the appropriate electronic structure of the solute molecule. This can be made, in principle, with the modern QM/MM method but is still impractical due to its huge computational demand. The decomposition mentioned above into the electrostatic and nonelectrostatic contributions[8] is much more difficult for the QM/MM method. A promising approach to tackle the problem is based on the reference interaction site model (RISM),[9,10] a statistical mechanics theory for molecular liquids. The theory has been extended to treat the nonequilibrium free energy profile,[11] which governs the electron-transfer reaction. The theory has also been combined with ab initio molecular orbital theories to determine the electronic structure of a solvated molecule (RISM−SCF).[12−14] In the preceding article (article 1),[15] we demonstrated that the combination of these two extensions is very useful for the purpose of determining the solvent reorganization energy ($\lambda_{s,C}$) associated with a charging process of a molecule in solution. In the present article, we apply the method to discuss the solvation process of *N*,*N*-dimethylaniline (DMA) and 1,4-

[†] Kyoto University.
[‡] Tohoku University.
[§] The Graduate University for Advanced Studies.
* To whom correspondence should be addressed.

10.1021/jp0371534 CCC: $27.50
Published on Web 07/02/2004

SCHEME 1: Schematic Illustration of the Free Energy Components Evaluation for $\lambda^0_{s,C}$ [a]

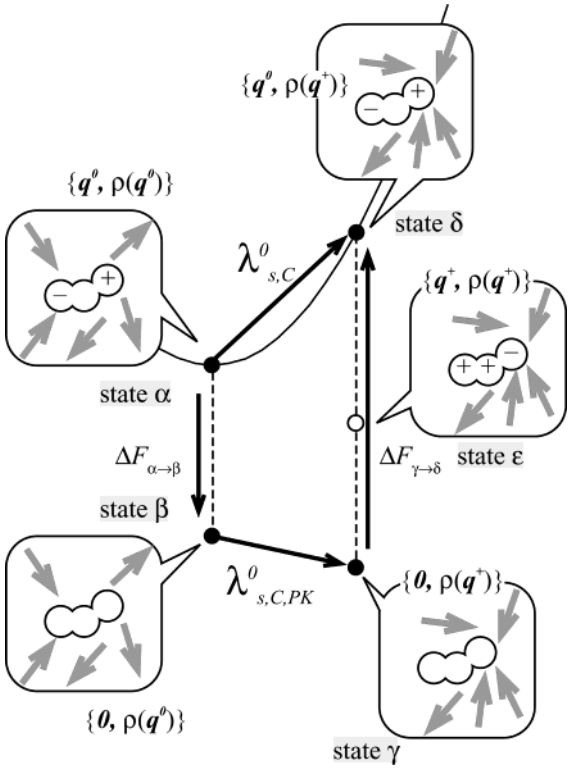

[a] A similar procedure can be employed for $\lambda^+_{s,C}$.

dimethoxybenzene (DMB) in acetonitrile solutions including the change in their electronic structure. A new scheme to decompose the solvent response to solute perturbation into the electrostatic and nonelectrostatic contributions is proposed to provide more insight into the solvent reorganization process. The organization of the present paper is as follows. Following a brief description of the method of decomposing the solvent reorganization energy into the electrostatic and nonelectrostatic contributions, the computational procedure is briefly reviewed in section 2. Geometric and electronic structures of DMB and DMB^+ are then discussed in section 3. Solvent reorganization energy, its components, and solvation structures in acetonitrile solutions are compared with those for DMA and DMA^+. Section 4 concludes the paper.

2. Methods

2.1. Dividing Procedure of the Solvent Reorganization Energy. It is of great interest to see what kind of solute−solvent interaction governs the reorganization process. $\lambda_{s,C}$ represents the free energy associated with the solvent reorganization. The quantity consists of two different contributions, namely, electrostatic and nonelectrostatic contributions. Because the RISM−SCF method and the detailed algebraic procedure to evaluate overall $\lambda_{s,C}$ have been described in the preceding paper,[14,15] only a brief review of the procedure is provided before the decomposition scheme of $\lambda_{s,C}$ into the two contributions is explained. In Scheme 1, thermodynamic states including both the charge distribution of solute and the solvent configuration are denoted by α, β, γ, δ, and ϵ. The charge distribution of the solute is depicted by + and − in the picture representing a solute. The solvent configuration is schematically represented by the thick arrows around the solute. The charge distributions and solvent configurations are also denoted by the two variables in the parenthesis: X in $\{X, \rho(Y)\}$ represents a state with charge distribution of solute molecule ($\mathbf{q}^0$ denotes neutral DMA or DMB, whereas $\mathbf{q}^+$ represents DMA^+ or DMB^+), and $\rho(Y)$ denotes the solvent configuration in equilibrium with the solute-charge distribution of Y. What we are primarily concerned with is the free energy change $\lambda^0_{s,C}$ associated with transition from the states α to δ, where state α is the equilibrium state, whereas the solvent configuration is not in equilibrium with the solute charge distribution in state δ. We assume that the "nonequilibrium" solvent configuration $\rho(\mathbf{q}^+)$ can be realized as an "equilibrium" state by putting charge $\mathbf{q}^+$ on the solute. State ϵ represents such an equilibrium state. We can evaluate $\lambda^0_{s,C}$ from the solvation free energy difference between the two equilibrium states (α and ϵ in the scheme, corresponding to $\Delta\mu^+ - \Delta\mu^0$) and from electrostatic energy change between states ϵ and δ. (See article 1 for more detail.)

$$\lambda^0_{s,C} = \Delta\mu^+ - \Delta\mu^0 - \mathbf{V}_+\cdot(\mathbf{q}^+ - \mathbf{q}^0) \tag{1}$$

where $\Delta\mu^0$ and $\Delta\mu^+$ are, respectively, the solvation free energies of the solute with charges $\mathbf{q}^0$ and $\mathbf{q}^+$. The solvation free energy can be calculated from the HNC approximation.[16]

$$\Delta\mu^0 = -\rho k_B T \sum_{ij} \int \mathrm{d}r \left[c^0_{ij}(r) - \frac{1}{2}(h^0_{ij}(r))^2 + \frac{1}{2} h^0_{ij}(r)\, c^0_{ij}(r) \right] \tag{2}$$

$$\Delta\mu^+ = -\rho k_B T \sum_{ij} \int \mathrm{d}r \left[c^+_{ij}(r) - \frac{1}{2}(h^+_{ij}(r))^2 + \frac{1}{2} h^+_{ij}(r)\, c^+_{ij}(r) \right] \tag{3}$$

These quantities are computed with sets of atomic charges ($\mathbf{q}^0$ and $\mathbf{q}^+$) obtained from the RISM−SCF wave functions of the solvated molecule. The electrostatic potential from solvent on these species are given by

$$(\mathbf{V}_0)_i = \rho \sum_j q^j_{\mathrm{solvent}} \int \mathrm{d}r\, 4\pi r^2 \frac{g^0_{ij}(r)}{r}, \tag{4}$$

$$(\mathbf{V}_+)_i = \rho \sum_j q^j_{\mathrm{solvent}} \int \mathrm{d}r\, 4\pi r^2 \frac{g^+_{ij}(r)}{r}. \tag{5}$$

Note that the electrostatic potentials $\mathbf{V}_0$ and $\mathbf{V}_+$ on the solute site are functions of thermodynamic states because $g^0_{ij}(r)$ and $g^+_{ij}(r)$ are the pair correlation functions (PCF) calculated with the respective charge distribution, $\mathbf{q}^0$ and $\mathbf{q}^+$. ρ and q^j_{solvent} represent the number density and the effective charge on the j-site (atom) of a solvent molecule, respectively.[15,17] This is the summary of the procedure given in article 1.

To divide $\lambda^0_{s,C}$ into the two contributions, i.e., electrostatic and nonelectrostatic, we introduce two hypothetical states, β and γ, in which all the charges in the solute molecule are removed and the solvent configurations are frozen. The solvent configuration in these states is different from each other, as are indicated by the arrows, and neither of them is in equilibrium with the solute charge state **0**. The free energy changes associated with the transition of the states from α to β, from β to γ, and from γ to δ are denoted, respectively, by $\Delta F_{\alpha\to\beta}$, $\lambda^0_{s,C,PK}$, and $\Delta F_{\gamma\to\delta}$. The thermodynamic cycle involving the new states gives the following relation,

$$\lambda^0_{s,C} = \Delta F_{\alpha\to\beta} + \lambda^0_{s,C,PK} + \Delta F_{\gamma\to\delta} \tag{6}$$

As is obvious from the scheme, the charges in the solute are not involved in the solvent reorganization process from state β to state γ. We therefore identify $\lambda^0_{s,C,PK}$ as the nonelectrostatic contribution to $\lambda^0_{s,C}$, and the rest as the electrostatic contribution $\lambda^0_{s,C,ES}$, that is,

$$\lambda^0_{s,C,ES} = \Delta F_{\alpha\to\beta} + \Delta F_{\gamma\to\delta} \tag{7}$$

We have used the notation $\lambda^0_{s,C,PK}$ for the nonelectrostatic contribution, because the solvent reorganization takes place under the influence of solute without charges, which is essentially a "packing" effect. Because the solvent configurations are fixed during the processes of changing the state from α to β, $\Delta F_{\alpha\to\beta}$ can be calculated from the following equation,[11]

$$\Delta F_{\alpha\to\beta} = \mathbf{V}_0\cdot(\mathbf{0} - \mathbf{q}^0) = -\mathbf{V}_0\cdot\mathbf{q}^0 \tag{8}$$

where **0** is a vector representing the all charges in solute sites being zero. $\Delta F_{\gamma\to\delta}$ can be obtained in a similar manner.

$$\Delta F_{\gamma\to\delta} = \mathbf{V}_+\cdot(\mathbf{q}^0 - \mathbf{0}) = \mathbf{V}_+\cdot\mathbf{q}^0 \tag{9}$$

and

$$\lambda^0_{s,C,ES} = \mathbf{V}_+\cdot\mathbf{q}^0 - \mathbf{V}_0\cdot\mathbf{q}^0 \tag{10}$$

$\lambda^0_{s,C,PK}$ can be obtained from eqs 1 and 6 by taking eqs 7−10 into account.

$$\lambda^0_{s,C,PK} = \Delta\mu^+ - \Delta\mu^0 - \mathbf{V}_+\cdot\mathbf{q}^+ + \mathbf{V}_0\cdot\mathbf{q}^0 \tag{11}$$

In the same way, the components for the cation ($\lambda^+_{s,C,PK}$ and $\lambda^+_{s,C,ES}$) can be computed as follows,

$$\lambda^+_{s,C} = \Delta\mu^0 - \Delta\mu^+ - \mathbf{V}_0\cdot(\mathbf{q}^0 - \mathbf{q}^+) = \lambda^+_{s,C,PK} + \lambda^+_{s,C,ES} \tag{12}$$

and

$$\lambda^+_{s,C,PK} = \Delta\mu^0 - \Delta\mu^+ - \mathbf{V}_0\cdot\mathbf{q}^0 + \mathbf{V}_+\cdot\mathbf{q}^+ = -\lambda^0_{s,C,PK}$$
$$\lambda^+_{s,C,ES} = \mathbf{V}_0\cdot\mathbf{q}^+ - \mathbf{V}_+\cdot\mathbf{q}^+ \tag{13}$$

It is noted that the absolute values of the nonelectrostatic contribution ($\lambda^{0/+}_{s,C,PK}$) are the same in the neutral and cationic species, but their signs are opposite due to an obvious physical reason. It is also noted that the electrostatic contribution ($\lambda^{0/+}_{s,C,ES}$) contains implicitly an entropy contribution of solvation, because $\mathbf{V}_{0/+}$ in the equation are computed from the total correlation function.

2.2. Computational Details. The electronic wave functions of solvated DMB and its cation (DMB^+) are computed by using the Hartree−Fock (HF) method with Dunning's (9s, 5p)/[3s, 2p] basis set augmented with a d-polarization function on the carbon, oxygen, and nitrogen atoms.[18]

All the molecules treated in the RISM theory are modeled with the all atom-type interaction including 20 sites for the solute and three sites for solvent acetonitrile.[19] The Lennard-Jones parameters of those molecules are taken from the literature[20] and are the same as those in the previous study[15] except for the oxygen atom ($\sigma = 3.0$ Å, $\epsilon = 0.17$ kcal mol^{-1}). All the van der Waals interactions between the solute and solvent are determined by means of the standard combination rule. The density of acetonitrile is assumed to be 0.011 39 molecule/Å^3 at 298.15 K.

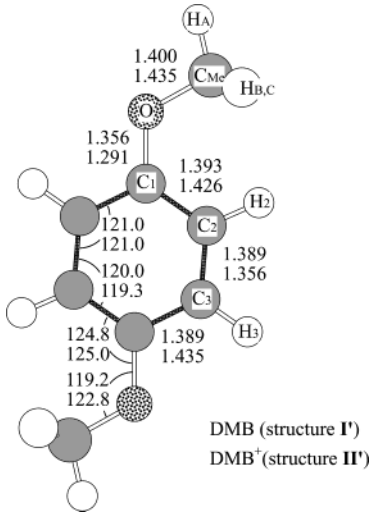

Figure 1. Selected geometrical parameters and atomic labeling in DMB and DMB^+ optimized structure under the C_{2h} symmetry: (upper) DMB (structure **I′**); (lower) DMB^+ (structure **II′**).

TABLE 1: Calculated Energy Components (kcal/mol) of DMB

	DMB		DMB^+	
	cis	trans	cis	trans
$\Delta E_{isolate}$	0.0[a]	0.4	0.0[a]	−0.4
E_{pol}[b]	0.5	0.3		0.2
$\Delta\mu$ (HNC)	11.6	14.0		−25.5

[a] Measured from −458.53789 hartree (DMB) and −458.29554 hartree (DMB^+). [b] $E_{pol} = E_{solute} - E_{isolate}$. See ref 17.

3. Results and Discussion

3.1. Characterization of the Geometry and Electronic Structure. The experimental data with respect to the structure of DMB is very limited: to our knowledge, only a measurement by X-ray crystallography has been performed,[21] in which the analysis was made on the basis of the trans planar conformation. Figure 1 shows the geometrical parameters and the atomic labeling in DMB and DMB^+ used in the present study. These geometries were optimized under the point group symmetry of C_{2h} in the gas phase. The parameters obtained for *trans*-DMB (structure **I′**) are in reasonable agreement with the X-ray data: the C_1−O bond length (1.36 Å) and the COC bond angle (119°) are remarkably close to the experimental data (1.36 Å and 121 ± 2°). On the other hand, computed and experimentally determined C−C bond lengths in the aromatic ring show a little difference. Three C−C bond lengths in the aromatic ring (C_1−C_2, C_2−C_3 and C_3−C_1) are similar in the computational results (∼1.39 Å), whereas they are quite different from each other in the X-ray results (1.36, 1.37, and 1.44 Å). It should be noted, however, that the optimized geometry in the present study is determined under the isolated condition and is not necessary to coincide with the solid state X-ray data. All the bond lengths are changed slightly upon the ionization to DMB^+ (structure **II′**): the lengths of C_{Me}−O and C_1−C_2 increase, whereas those of O−C_1 and C_2−C_3 decrease. This may suggest that character of the benzene nucleus in DMB^+ is altered to a *p*-quinone-like one, though the change is small.

Table 1 lists the energy components obtained in the present study.[17] Tzeng et al. reported that the computed energy

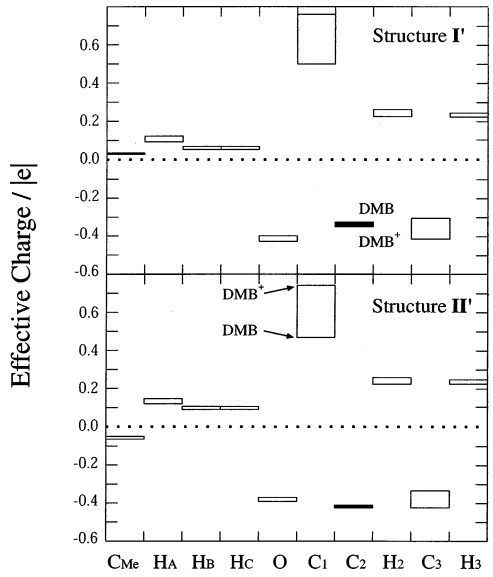

Figure 2. Effective charges and their changes in the ionization process (DMB → DMB$^+$). Open and filled squares, respectively, show electron gain and loss, and the top and bottom of squares indicate the effective charge in the individual atomic site of DMB and DMB$^+$.

difference between *cis*- and *trans*-DMB isomers is very small (∼0.3 kcal/mol),[22] and several conformers should coexist under a realistic condition. Our result on the energy difference in the gas phase shows good accord with their report. The relative stability reverses in DMB$^+$, and the trans form is slightly stable in energy than the cis form. We then carried out the computation in the solution phase on the *cis*- and *trans*-DMB by using the RISM−SCF method, and found that the free energy difference between them is slightly greater than that in the gas phase.[23] It is very likely that the methoxy group rotation does not affect the solvation profile. All the PCFs in the two isomers are, in fact, almost identical. Therefore, we shall concentrate our discussion only on the trans form of DMB and DMB$^+$ in the present article, which corresponds to the experimental analysis.

In Figure 2, effective charges and their changes upon the ionization (DMB → DMB$^+$) in acetonitrile solution computed with the RISM−SCF method are shown. The charges are derived from the electrostatic potential (ESP) fitting procedure. The graph should be interpreted by the same way in our previous article:[15] The open squares symbolize an increase in the positive charge or loss of electrons at the atomic sites indicated by the *x*-axis, and the filled squares represent the gain of electrons. The top and bottom edges of the square correspond to the effective charge in DMB and DMB$^+$. For example, the charge changes from the bottom to top edges at the C_1-site upon ionization (DMB → DMB$^+$), whereas it changes from the top to bottom edges in the C_2-site in both structures I′ and II′. It is very interesting that the most remarkable change of the charge is found in C_1, whereas the charges in the other atoms do not change so much. The changing profiles in the upper panel (structure **I′**) and the lower one (structure **II′**) look very similar, indicating the change in the effective charge (or electronic structure) is not sensitive to the geometry, which is in noticeable contrast to the DMA case. This is related to a fact that the geometrical alternation upon the ionization is insignificant in the DMB case compared to DMA.[24] The deviation of the dimethylamino group in DMA from the planer conformation due to the wagging motion, which is the main geometrical difference between DMA and DMA$^+$, isolating the lone pair electrons of the N atom from the resonating electrons in the benzene ring.[15,25]

TABLE 2: Computed Reorganization Energy (eV) $\lambda_{s,C}$ [26]

		λ_s(DMB)			λ_s(DMA)		
		$\lambda_{s,C,PK}$	$\lambda_{s,C,ES}$	total	$\lambda_{s,C,PK}$	$\lambda_{s,C,ES}$	total
$\lambda^0_{s,C}$	structure **I/I′**	1.62	0.22	1.84	1.79	0.08	1.88
	structure **II/II′**	1.56	0.27	1.84	1.63	0.20	1.82
$\lambda^+_{s,C}$	structure **I/I′**	−1.62	3.42	1.80	−1.79	3.62	1.82
height	structure **II/II′**	−1.56	3.36	1.79	−1.63	3.41	1.78

3.2. Solvent Reorganization Energy and Its Components. In the previous study, we showed that electronic structure change of DMA upon ionization strongly couples with the wagging motion (antipyramidalization) of dimethylamino group, and the solvation process can be well understood in terms of the linear response theory. The solvent reorganization energies associated with a charging process ($\lambda_{s,C}$) computed by eq 2 are listed in Table 2. They are similar with those of DMA and DMA$^+$ discussed in the previous article.[15] $\lambda_{s,C}$ is insensitive to the substitution of the amino group to dimethoxy group. A direct comparison between theoretical and the TR-EPR experimental results[2] cannot be made, because the former does not include the contribution from anion species and from the interaction between the donor and acceptor. It is possible, however, to compare the trends with experimental results in which the same acceptor is used, because the difference in the donor−acceptor interactions between DMA and DMB systems is expected to be small. Though the system studied by the theory is slightly different from that observed by the experiment, trimethoxybenzene instead of dimethoxybenzene, the theoretical result is in good harmony with the experimental results in which λ_s for the two molecules are quite similar. More direct comparison can be made with $\lambda^{CMD}_{s,C}$ evaluated by the simple Born model.

$$\lambda^{CMD}_{s,C} = \frac{1}{2}\left(\frac{1}{x} - \frac{1}{\epsilon_S}\right)\frac{1}{r_D} \tag{14}$$

where $x = \epsilon_{OP}$ (model A) or 1 (model B). We use the parameter that best reproduces the experimental results of λ_s,[2d] $\epsilon_{OP} = 1.8$, $\epsilon_S = 37.3$, and $r_D = 3.47$ Å (DMA). Unfortunately, r_D for DMB is not available, thereby the corresponding value for 1,2,4-trimethoxybenzene, 3.69 Å, is used. $\lambda^{CMD}_{s,C}$ by models A and B for DMA are, respectively, 1.10 and 2.02 eV and those for DMB are 1.03 and 1.90 eV.[26] Estimations by the present model shown in the table are intermediate between those by model A and B. Again, the substitution effect is not significant in the present systems, although the $\lambda_{s,C}$ for DMA is slightly greater than that for DMB. The difference might be related to the polarization energy of TMPD (*N*,*N*,*N*′,*N*′-tetramethyl-*p*-phenylenediamine), in which a spontaneous ionization process from the S_1 state was studied in detail.[27]

It is worthwhile to emphasize again that the present results are obtained on the basis of an ab initio model that does not include any adjustable parameters, whereas the Born model includes several parameters, such as r_D, to be adjusted to experimental results. Although the two methods give apparently similar results for the solvent reorganization energy, the level of description is entirely different: the present method is obviously superior to the Born method in the sense that it does not use any adjustable parameters. The table also includes the electrostatic and nonelectrostatic contributions to $\lambda_{s,C}$. The ingredients for the neutral and cationic species are quite different even though the overall $\lambda_{s,C}$'s are close each other: the contribution from the nonelectrostatic effect ($\lambda_{s,C,PK}$) is comparable to that from the electrostatic contribution ($\lambda_{s,C,ES}$) in the neutral species, whereas $\lambda_{s,C,ES}$ dominates in the ionic species.

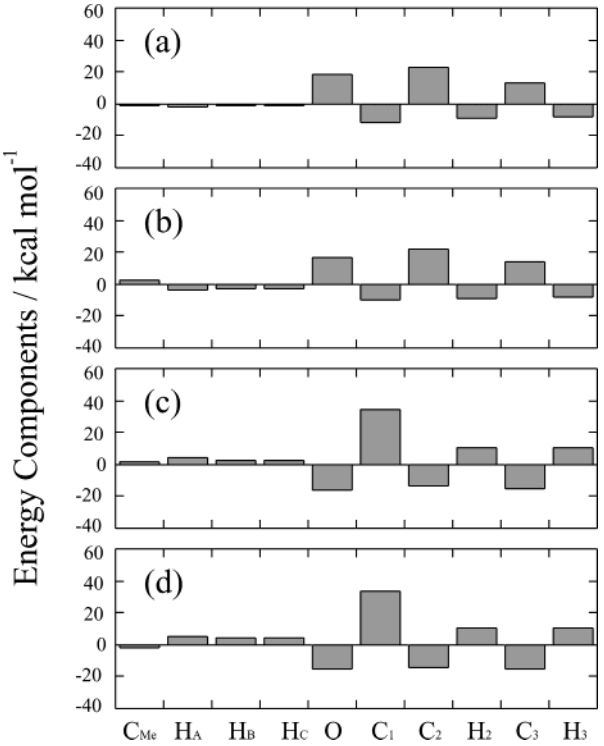

Figure 3. Contributions to $\lambda_{s,C}$ from individual atomic site in DMB/DMB$^+$: (a) DMB in structure **I′**; (b) DMB in structure **II′**; (c) DMB$^+$ in structure **I′**; (d) DMB$^+$ in structure **II′**.

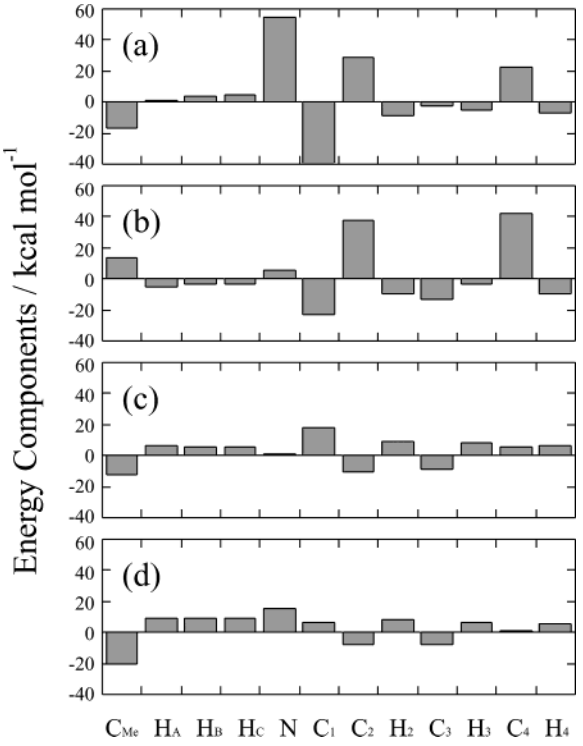

Figure 4. Contributions to $\lambda_{s,C}$ assigned to individual atomic site in DMA/DMA$^+$: (a) DMA in structure **I**; (b) DMA in structure **II**; (c) DMA$^+$ in structure **I**; (d) DMA$^+$ in structure **II**.

This is consistent with our intuitive consideration on the solvation processes as well as with the previous studies,[28] suggesting that the decomposing procedure presented here makes sense. The signs of the two contributions are always opposite in the cation species, in other words, they tend to work complementarily. On the basis of a very naive consideration, this can be understood, for example, in terms of an overlap of solute and solvent molecules caused by translational and rotational motions: bringing the solute and solvent molecules into closer distance gives rise to stabilization in terms of the electrostatic energy but, at the same time, increases the nonelectrostatic interaction energy.[29] The importance of nonelectrostatic contribution found here cannot be realized by the macroscopic Marcus model in which $\lambda_{s,C}$ is treated only on the basis of the electrostatic interaction.[30]

$\lambda_{s,C}$ can be "formally" decomposed into contributions from atoms (α) consisting of the solute molecule.[15]

$$\lambda^0_{s,C} = \sum_\alpha \lambda^0_{s,\alpha}$$

$$\lambda^+_{s,C} = \sum_\alpha \lambda^+_{s,\alpha} \qquad (15)$$

and

$$\lambda^0_{s,C,\alpha} = \Delta\mu^+_\alpha - \Delta\mu^0_\alpha - (\mathbf{V}_+)_\alpha(\Delta\mathbf{q})_\alpha$$

$$\lambda^+_{s,C,\alpha} = \Delta\mu^0_\alpha - \Delta\mu^+_\alpha + (\mathbf{V}_0)_\alpha(\Delta\mathbf{q})_\alpha \qquad (16)$$

Figure 3 shows the components with respect to the two optimized geometry of DMB (structure **I′** and **II′**). By comparing (a) with (b), or (c) with (d), one can notice that the geometrical change, which is actually small, does not affect $\lambda_{s,C}$ as well as their components. It is very interesting that $\lambda_{s,C}$ consists of positive and negative contributions, indicating that the process (DMB $\rightarrow$ DMB$^+$ or DMB$^+$ $\rightarrow$ DMB) contains both the solvation and the desolvation in atomic level: some atoms (e.g., C_1) of the solute prefer the solvation structure around DMB to that around DMB$^+$, whereas the other atoms (e.g., C_2, C_3, and O) prefer the structure around DMB$^+$ (DMB). It is noted that the situation is very different in the case of DMA and DMA$^+$, in which the components of $\lambda_{s,C}$ show characteristic behavior, especially in the amino group (Figure 4). In the structure of optimized DMA (structure **I**), contributions from the N-site, C_2-site, and C_4-site are noticeably large compared to those from other sites, Figure 4a, whereas the contribution from the N-site virtually disappears in the optimized structure of the cation (structure **II**) (Figure 4b). The wagging motion of the amino group, which is an essential cause of the difference between the two structures, reduces the contribution from the N-site. Physicochemical origin of $\lambda_{s,C}$ in DMA$^+$ (Figures 4c,d) is significantly different from that in the neutral species: there is no distinct site to contribute to the overall $\lambda_{s,C}$ and all the sites participate evenly. It is noteworthy to point out that origin of $\lambda_{s,C}$ in atomic level could be quite different, even though the overall $\lambda_{s,C}$ is almost identical.

Each decomposed $\lambda_{s,C,\alpha}$ can be further divided into two contributions, namely the electrostatic and nonelectrostatic ones by using the aforementioned scheme. The results are shown in Figure 5 (DMB and DMB$^+$) and 6 (DMA and DMA$^+$). Similar trends found in the division of overall $\lambda_{s,C}$ are seen in these figures: the two contributions participate with the opposite signs. The nonelectrostatic contribution dominates in the neutral species, whereas the electrostatic one is important in the cation. It is very interesting that the C_1 site in DMB$^+$ makes large contributions due to the remarkable change of its charge (see Figure 2). In the case of DMA$^+$, the contribution governing the $\lambda_{s,C}$ is localized around the amino group (Figure 6 c,d), and the importance of N-site and C_1-site strongly depends on the geometrical change.

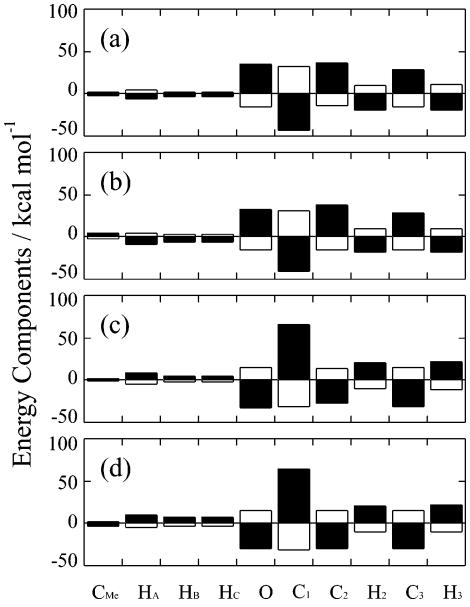

Figure 5. Contributions to $\lambda_{s,C}$ from individual atomic site in DMB/DMB$^+$. Shading indicates the electrostatic contribution, and no shading the nonelectrostatic one: (a) DMB in structure **I′**; (b) DMB in structure **II′**; (c) DMB$^+$ in structure **I′**; (d) DMB$^+$ in structure **II′**.

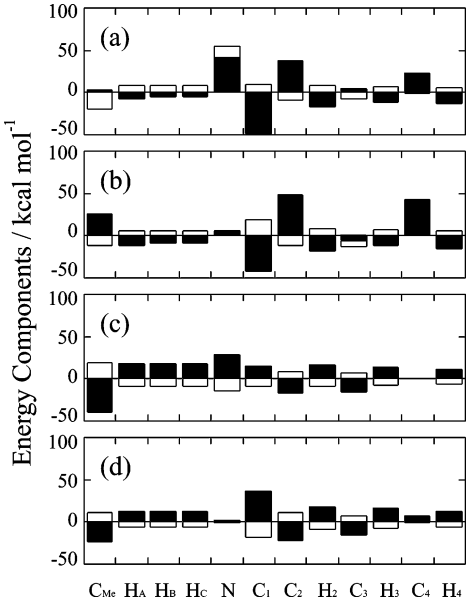

Figure 6. Contributions to $\lambda_{s,C}$ assigned to individual atomic site in DMA/DMA$^+$: (a) DMA in structure **I**; (b) DMA in structure **II**; (c) DMA$^+$ in structure **I**; (d) DMA$^+$ in structure **II**. See the footnote in Figure 4.

3.3. Solvation Structure. The solvation structure is represented in terms of a set of pair correlation functions (PCFs) that are obtained from the RISM−SCF theory. PCFs between atoms in solvent acetonitrile and two selected atoms of DMB/DMB$^+$ molecules are shown in Figure 7, (a) C_{Me} in methoxy group and (b) C_1. (See Figure 1 for the labeling.)

We tried to figure out the most plausible solvation structure (MPSS)[31] to understand the solvation profile. However, the result indicates a mixture of a large number of solvent configurations: any preferential solvent configuration that fits perfectly to the set of PCFs was not found. An example is the PCF around the C_{Me} shown in Figure 7a. There is no configuration of acetonitrile molecules, which is consistent with all the first peak positions in the PCFs of the three pairs of atoms: Me−C_{Me} at 3.7 Å, C−C_{Me} at 4.0 Å, and N−C_{Me} at 3.4 Å. A

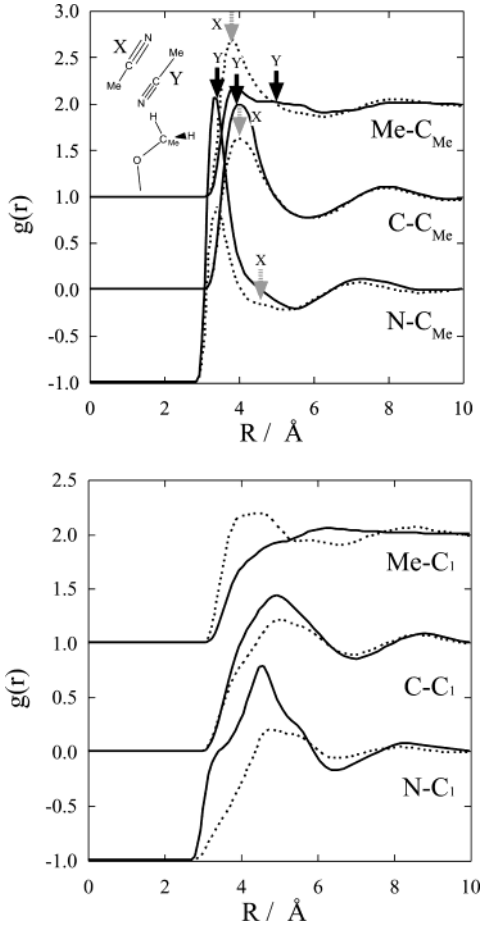

Figure 7. (a) Pair correlation functions around DMB (dotted lines) and DMB$^+$ (solid lines) between C_{Me} and solvent acetonitrile. A schematic view of the two typical solvent confiurations (**X** and **Y**) of acetonitrile are depicted in the figure. The arrows indicate the atomic distances where the largest peaks are expected to be observed, if the solvent configurations are **X** or **Y**. (b) Pair correlation functions around DMB (dotted lines) and DMB$^+$ (solid lines) between C_1 (α carbon) and solvent acetonitrile.

possible interpretation of these PCFs is that they are attributable to a few different coordination structures. A schematic view of the two typical solvent confiurations (**X** and **Y**) of acetonitrile are depicted in the figure. The arrows indicate the atomic distances where the largest peaks are expected to be observed, if the solvent configurations are **X** or **Y**. The positions of the first peaks of Me-C_{Me} and C−C_{Me} for DMB show good agreement with those estimated from the geometric consideration assuming the **X** configuration, indicating the **X** is dominant for the solute. Similarly, the positions of the first peaks of C−C_{Me} and N−C_{Me} for DMB$^+$ show good agreement with those estimated from the geometric consideration assuming the **Y** configuration, indicating the **Y** is dominant for the solute. There are no large peaks for N−C_{Me} at the position corresponding to the **X** configuration. Similarly, there are no large peaks for Me−C_{Me} at the position corresponding to the **Y** configuration. We observe only discernible shoulders at those positions. Apparently, the solvation of **X** is dominant in DMB and it becomes less important upon the ionization; namely, the configuration **Y** takes over in DMB$^+$. It is noted that the changes of the peak height suggest that the both solvation structures coexist and only their probability ratio changes upon the ionization.

The peak positions of the PCFs in DMA and their changes upon the ionization are very similar to those of DMB (not shown here). It is noteworthy that even the PCFs around the hetero-

atoms (O or N) look very similar in the two molecules. It is considered that because of the absence of specific interactions such as the hydrogen bond, a relatively weak electrostatic interaction primarily governs the solute−solvent interaction, and the shape difference between DMA and DMB owing to the substitution is not essential to the solvation profile. This may answer the question why the Marcus theory, which is based on the continuum dielectric model and ignores detailed solvation structure, is a good model to estimate the solvent reorganization energies, $\lambda_{s,C}$. Whether or not the Marcus theory with the continuum dielectric model is successful as well for the system in which specific interactions are important should be examined carefully.

4. Conclusions

We have proposed a new procedure that can realize the decomposition of solvent reorganization energy associated with a charging process, $\lambda_{s,C}$, into two types of contributions, namely electrostatic and nonelectrostatic contributions from the first principle. The method used here is based on a combination of the ab initio RISM−SCF theory and the method proposed by Chong et al. to evaluate the nonequilibrium free energy associated with the electron-transfer reaction, which we have proposed very recently. The new decomposition procedure is also combined with a method proposed in the preceding article (article 1), in which $\lambda_{s,C}$ is partitioned into contributions from each atom composing the solute molecule.

All these methods were applied to compare the solvation process of two different molecules (DMA, DMB, and their cation). We found the computed $\lambda_{s,C}$'s give consistent results with the recent TR-EPR experiment, demonstrating the superiority of the new method. Structural information on the solvation process can be obtained in molecular detail by analyzing the PCFs. The experimentally observed λ_s for DMA and DMB were very close, and the present computational study reproduces the trend reasonably well. At the same time, the decomposition procedure reveals that the physical origins of $\lambda_{s,C}$ are very different from each other at the molecular level. The analysis on PCFs indicates that solvation structures in the DMA and DMB systems are similar, and there are no conspicuous characters. The loose solvation structures found in both systems could be the reason the Marcus model is applicable for these molecular systems. This is, however, not a common phenomenon seen in any solute−solvent system. A specific interaction such as hydrogen bonding can considerably affect $\lambda_{s,C}$ (or λ_s) and its components. In the forthcoming article, we will present such an example.

Acknowledgment. We gratefully acknowledge Dr. Ryo Akiyama (Kyushu University) for invaluable discussion. H.S. thanks Prof. Shigeyoshi Sakaki (Kyoto University) for his encouragement. This research was supported by the Grant-in-Aid for Encouragement of Young Scientists, and from the Japanese Ministry of Education, Science, Sports, and Culture (MONBU SHO).

References and Notes

(1) (a) Marcus, R. A. *J. Chem. Phys.* **1956**, *24*, 966. (b) Masuhara, H.; Mataga, N. *Acc. Chem. Res.* **1981**, *14*, 312. (c) Marcus, R. A.; Sutin, N. *Biochim. Biophys. Acta* **1985**, *811*, 265. (d) Kavarnos, G. J.; Turro, N. J. *Chem. Rev.* **1986**, *86*, 401.

(2) (a) Kobori, Y.; Yago, T.; Akiyama, K.; Tero-Kubota, S. *J. Am. Chem. Soc.* **2001**, *123*, 9722. (b) Kobori, Y.; Akiyama, K.; Tero-Kubota, S. *J. Chem. Phys*. **2000**, *113*, 465. (c) Kobori, Y.; Akiyama, K.; Tero-Kubota, S. *J. Phys. Chem. A* **1999**, *103*, 5416. (d) Kobori, Y.; Zikihara, K.; Yago, T.; Akiyama, K.; Sato, H.; Hirata F.; Tero-Kubota, S. unpublished.

(3) (a) Basilevsky, M. V.; Chudinov, G. E.; Newton, M. D. *Chem. Phys.* **1994**, *179*, 263. (b) Newton, M. D.; Basilevsky, M. V.; Rostov, I. V. *Chem. Phys.* **1998**, *232*, 201. (c) Liu, Y.-P.; Newton, M. D. *J. Phys. Chem.* **1995**, *99*, 12382. (d) Kumar, K.; Kurnikov, I. V.; Beratan, D. N.; Waldeck, D. H.; Zimmt, M. B. *J. Phys. Chem. A* **1998**, *102*, 5529.

(4) (a) Rostov, I. V.; Basilevsky, M. V.; Newton, M. D. In *Simulation and Theory of Electrostatic Interactions in Solution*; Pratt, L. R., Hummer, G., Eds.; AIP, 1999. (b) Zimmt, M. B.; Waldek, D. H. *J. Phys. Chem. A* **2003**, *107*, 3580. (c) Hammes-Schiffer, S. *Acc. Chem. Res.* **2001**, *34*, 273.

(5) (a) Ungar, L. W.; Newton, M. D.; Voth, G. A. *J. Phys. Chem. B* **1999**, *103*, 7367. (b) Ando, K. *J. Chem. Phys.* **2001**, *115*, 5228. (c) Leontyev, I. V.; Vener, M. V.; Rostov, I. V.; Basilevsky, M. V.; Newton, M. D. *J. Chem. Phys.* **2003**, *119*, 8024. (d) Perng, B.-C.; Newton, M. D.; Raineri, F. O.; Friedman, H. L. *J. Chem. Phys.* **1996**, *104*, 7177.

(6) (a) Basilevsky, M. V.; Chudinov, G. E.; Napolov, D. V. *J. Phys. Chem.* **1993**, *97*, 3270. (b) Basilevsky, M. V.; Chudinov, G. E.; Rostov, I. V.; Liu, Y.-P.; Newton, M. D. *J. Molec Struct. (THEOCHEM)* **1996**, *371*, 191. (c) Truhlar, D. G.; Schenter, G. K.; Garrett, B. C. *J. Chem. Phys*. **1993**, *98*, 5756.

(7) (a) Bader, J. S.; Cortis, C. M.; Berne, B. J. *J. Chem. Phys.* **1997**, *106*, 2372. (b) Bader, J. S.; Berne, B. J. *J. Chem. Phys.* **1996**, *104*, 1293.

(8) Levy, R. M.; Gallicchio, E. *Annu. Rev. Phys. Chem.* **1998**, *49*, 531.

(9) Chandler, D.; Andersen, H. C. *J. Chem. Phys.* **1972**, *57*, 1930.

(10) (a) Hirata, F.; Rossky, P. *J. Chem. Phys. Lett.* **1981**, *83*, 329. (b) Hirata, F.; Pettitt B. M.; Rossky, P. J. *J. Chem. Phys.* **1982**, *77*, 509. (c) Hirata, F.; Rossky P. J.; Pettitt, B. M. *J. Chem. Phys.* **1983**, *78*, 4133.

(11) (a) Chong, S.-H.; Miura, S.; Basu, G.; Hirata, F. *J. Phys. Chem.* **1995**, *99*, 10526. (b) Chong, S.-H.; Hirata, F. *Mol. Simul.* **1996**, *16*, 3. (c) Chong, S.-H.; Hirata, F. *J. Chem. Phys.* **1997**, *106*, 5225. (d) Chong, S.-H.; Hirata, F. *Chem. Phys. Lett.* **1998**, *293*, 119. (e) Akiyama, R.; Kinoshita, M.; Hirata, F. *Chem. Phys. Lett.* **1999**, *305*, 251.

(12) Ten-no, S.; Hirata, F.; Kato, S. *J. Chem. Phys.* **1994**, *100*, 7443.

(13) Sato, H.; Hirata, F.; Kato, S. *J. Chem. Phys.* **1996**, *105*, 1546.

(14) Sato, H.; Hirata, F. *J. Phys. Chem. A* **2002**, *106*, 2300.

(15) Sato, H.; Kobori, Y.; Tero-Kubota, S.; Hirata, F. *J. Chem. Phys.* **2003**, *119*, 273.

(16) Singer, S. J.; Chandler, D. *Mol. Phys.* **1985**, *55*, 621.

(17) The electronic polarization energy of the solute (E_{pol}) in this article corresponds to the solute reorganization energy E_{reorg} in our previous studies. We use E_{pol} to avoid confusion with the solvent reorganization (λ_s), as well as to make clear that the nuclear positions of the solute molecule are fixed upon transferring from the gas phase to the acetonitrile solutions.

(18) (a) Huzinaga, S. *J. Chem. Phys.* **1965**, *42*, 1293. (b) Dunning, T. H. *J. Chem. Phys.* **1970**, *53*, 2823.

(19) Jorgensen, W. L.; Briggs, J. M. *Mol. Phys.* **1988**, *63*, 547.

(20) Jorgensen, W. L.; Laird, E. R.; Nguyen T. B.; Tirado-Rives, J. *J. Comput. Chem.* **1993**, *14*, 206.

(21) Goodwin, T. H.; Przybylska, M.; Robertson, M. *Acta Crystallogr.* **1950**, *3*, 279.

(22) Tzeng, W. B.; Narayanan, K.; Hsieh, C. Y.; Tung, C. C. *J. Mol. Struct.* **1998**, *448*, 91.

(23) It is desired to confirm that the solvation structures of *trans*-DMB^+ and *cis*-DMB^+ are similar. But the convergence of the RISM−SCF computation for *cis*-DMB^+, unfortunately, was not attained.

(24) Rettig, W.; Zietz, B. *Chem. Phys. Lett.* **2000**, *317*, 187.

(25) The electronic structure of DMA with structure **I** is adequately represented as only the left-hand side one among the three resonance structures given in the Scheme 1 of ref 15. Note that the arrow of the left-hand side in the lower panel (structure **I**) of this scheme is thin compared to the other arrows. The situation is different in the upper panel (structure **II**), because of its geometrical difference in dimethylamino group.

(26) The related experimental λ_s [2d] is 1.39 eV (*N*,*N*-dimethylaniline with duroquinone in C_3H_7CN solvent) and 1.33 eV (1,2,4-trimethoxybenzene with duroquinone in C_3H_7CN solvent).

(27) (a) Katoh, R.; Lacmann, K.; Schmidt, W. F. *Chem. Phys.* **1995**, *195*, 457. (b) Hirata, Y.; Ichikawa, M.; Mataga, N. *J. Phys. Chem.* **1990**, *94*, 3872.

(28) Aherne, D.; Tran, V.; Benjamin J. Schwartz, B. J. *J. Phys. Chem. B* **2000**, *104*, 5382.

(29) Rick, S. W.; Berne, B. J. *J. Am. Chem. Soc.* **1994**, *116*, 3949.

(30) (a) Berg, M. *Chem. Phys. Lett.* **1998**, *228*, 317. (b) Bagchi, B. *J. Chem. Phys.* **1994**, *100*, 6658.

(31) Sato H.; Hirata, F. *Bull. Chem. Soc. Jpn.* **2001**, *74*, 1831.